DNA methylation analysis of Homeobox genes implicates *HOXB7* hypomethylation as risk factor for neural tube defects

Anne Rochtus, Benedetta Izzi, Elise Vangeel, Sophie Louwette, Christine Wittevrongel, Diether Lambrechts, Yves Moreau, Raf Winand, Carla Verpoorten, Katrien Jansen, Chris Van Geet, and Kathleen Freson

QUERY SHEET

This page lists questions we have about your paper. The numbers displayed at left can be found in the text of the paper for reference. In addition, please review your paper as a whole for correctness.

Q1. Au: Please confirm you have submitted your publication costs form.
Q2. Au: Please provide missing keywords.
Q3. Au: Please provide the complete bibliographic details for Ref. [40].

TABLE OF CONTENTS LISTING

The table of contents for the journal will list your paper exactly as it appears below:

DNA methylation analysis of Homeobox genes implicates *HOXB7* hypomethylation as risk factor for neural tube defects
Anne Rochtus, Benedetta Izzi, Elise Vangeel, Sophie Louwette, Christine Wittevrongel, Diether Lambrechts, Yves Moreau, Raf Winand, Carla Verpoorten, Katrien Jansen, Chris Van Geet, and Kathleen Freson

RESEARCH PAPER

Epigenetics 0:0, 1–10; January 1, 2015; © 2015 Taylor & Francis Group, LLC

DNA methylation analysis of Homeobox genes implicates *HOXB7* hypomethylation as risk factor for neural tube defects

Anne Rochtus[1,2], Benedetta Izzi[1], Elise Vangeel[3], Sophie Louwette[1], Christine Wittevrongel[1], Diether Lambrechts[4,5], Yves Moreau[6], Raf Winand[6], Carla Verpoorten[2], Katrien Jansen[2], Chris Van Geet[1,2], and Kathleen Freson[1,*]

[1]Department of Cardiovascular Sciences; Center for Molecular and Vascular Biology; University of Leuven; Leuven, Belgium; [2]Department of Pediatrics; University Hospitals Leuven; Leuven, Belgium; [3]Genetic Research About Stress and Psychiatry (GRASP); University of Leuven; Leuven, Belgium; [4]Vesalius Research Center; VIB; Leuven, Belgium; [5]Laboratory for Translational Genetics; Department of Oncology; University of Leuven; Leuven, Belgium; [6]Department of Electrical Engineering ESAT-SCD; University of Leuven; Leuven, Belgium

Neural tube defects (NTDs) are common birth defects of complex etiology. Though family- and population-based studies have confirmed a genetic component, the responsible genes for NTDs are still largely unknown. Based on the hypothesis that folic acid prevents NTDs by stimulating methylation reactions, epigenetic factors, such as DNA methylation, are predicted to be involved in NTDs. Homeobox (*HOX*) genes play a role in spinal cord development and are tightly regulated in a spatiotemporal and collinear manner, partly by epigenetic modifications. We have quantified DNA methylation for the different *HOX* genes by subtracting values from a genome-wide methylation analysis using leukocyte DNA from 10 myelomeningocele (MMC) patients and 6 healthy controls. From the 1575 CpGs profiled for the 4 *HOX* clusters, 26 CpGs were differentially methylated (*P*-value < 0.05; β-difference > 0.05) between MMC patients and controls. Seventy-seven percent of these CpGs were located in the *HOXA* and *HOXB* clusters, with the most profound difference for 3 CpGs within the *HOXB7* gene body. A validation case-control study including 83 MMC patients and 30 unrelated healthy controls confirmed a significant association between MMC and *HOXB7* hypomethylation (-14.4%; 95% CI: 11.9–16.9%; *P*-value < 0.0001) independent of the *MTFHR 667C>T* genotype. Significant *HOXB7* hypomethylation was also present in 12 unaffected siblings, each related to a MMC patient, suggestive of an epigenetic change induced by the mother. The inclusion of a neural tube formation model using zebrafish showed that Hoxb7a overexpression but not depletion resulted in deformed body axes with dysmorphic neural tube formation. Our results implicate *HOXB7* hypomethylation as risk factor for NTDs and highlight the importance for future genome-wide DNA methylation analyses without preselecting candidate pathways.

Introduction

Neural tube defects (NTDs), affecting 0.5–2 per 1000 pregnancies, arise as a failure of the neural tube to close in the cranial (anencephaly) or the caudal (myelomeningocele) region. [1-3] The nature and severity of NTDs is determined by the stage and axial level at which closure fails. Cranial NTDs are mostly not compatible with life, while caudal NTDs give rise to lifelong disabilities. Although more than 250 genes are known to cause NTDs in mice [4,5] and many candidate genes have been studied in patient cohorts, the molecular basis underlying NTDs still remains largely unknown. Folic acid reduced the incidence of NTDs by 50–75%. [6] However, in most NTD-affected pregnancies maternal folic acid levels are within the normal range [7] and, despite optimal supplementation, a significant proportion of NTDs are unresponsive to folic acid. [6,8] This would suggest the existence of folic acid resistance in mothers at risk for NTD-affected pregnancies, but this hypothesis is not supported by genetic and/or environmental risk factors. Folic acid is central to the one-carbon metabolism that produces pyrimidines and purines for DNA synthesis and for the generation of S-adenosyL-methionine, which is a methyl donor for DNA, RNA, and protein methylation. The only well-characterized genetic risk factor for NTDs is the *677C>T* variant in the 5,10-methylene tetrahydrofolate reductase gene *(MTHFR)*, causing thermolability of the enzyme and predicted to divert the available methyl groups from the DNA methylation toward the DNA synthesis pathway. [6] Interestingly, the *MTHFR 677C>T* variant is associated with global DNA hypomethylation in both controls and NTDs,[6,9] and this seems to be more pronounced under low folic acid conditions. [10] Most DNA methylation studies in patients with NTDs were performed independently of the presence of the *MTHFR 677C>T* variant. Findings of global DNA and *LINE-1* hypomethylation were found in fetal neural tissue DNA from NTD patients, suggesting that disruption of genomic stability may lead to abnormal neural tube closure. [11,12]

*Correspondence to: Kathleen Freson; Email: freson@med.kuleuven.be
Submitted: 09/26/2014; Revised: 11/27/2014; Accepted: 12/07/2014
http://dx.doi.org/10.1080/15592294.2014.998531

Table 1 Background information of MMC patients included in the HumanMethylation450 BeadChip and Sequenom EpiTYPER

MMC patient	Type MMC	Hy/VP	ACM	Scoliosis	ADL	UI	Ethnicity	Maternal age (years) at birth of MMC patient	MMC patient		Sibling		MMC patient versus sibling age (months)
									MTHFR 677C>T	Gender	MTHFR 677C>T	Gender	
1*+	S	yes	1	yes	2	yes	Belgian	36	CC	F			
2*+	LS	yes	2	yes	3	yes	Belgian	29	CT	F			
3*+	LS	yes	2	yes	3	yes	Moroccan	32	CT	M			
4*+	LS	yes	1	yes	3	yes	Indonesian	26	CC	F			
5*+	LS	yes	2	no	2	yes	Belgian		CC	M	CC	F	−18
6*+	LS	yes	2	yes	3	yes	Belgian	27	CC	F			
7*+	LS	yes	1	yes	3	yes	Belgian		CC	M			
8*+	S	yes	2	no	1	yes	Belgian	27	CC	F			
9*	S	no	0	no	1	yes	Belgian		TT	M			
10*	LS	yes	2	no	2	yes	Belgian	25	CC	M			
11+	LS	yes	2	yes	3	yes	Belgian	27	CC	M			
12+	LS	yes	2	yes	3	yes	Turkish	28	CC	F			
13+	S	yes	0	no	1	yes	Belgian	33	CT	M			
14+	LS	yes	2	yes	3	yes	Belgian		CC	F			
15+	LS	yes	2	yes	3	yes	Turkish	20	CT	F			
16+	S	yes	2	yes	3	yes	Belgian		TT	M			
17+	LS	yes	2	yes	3	yes	Belgian	25	CT	F			
18+	S	yes	2	yes	2	yes	Belgian	28	CC	M			
19+	LS	yes	2	no	1	yes	Belgian	36	CT	M			
20+	LS	yes	2	yes	1	yes	Belgian		CT	M			
21+	LS	yes	2	yes	3	yes	Belgian	36	CT	F			
22+	TL & LS	yes	2	yes	3	yes	Belgian	23	CC	M			
23+	S	no	0	yes	1	yes	Belgian	30	CT	M			
24+	LS	yes	2	yes	2	yes	Belgian	25	CT	F			
25+	LS	yes	2	no	2	yes	Belgian	34	CC	F			
26+	LS	no	0	no	1	yes	Belgian		CC	F			
27+	LS	yes	2	yes	3	yes	Belgian		CT	M	CC	F	−20
28+	LS	yes	2	yes	3	yes	Moroccan		CT	F			
29+	LS	yes	2	yes	3	yes	Belgian	31	CC	M	CC	M	−19
30+	LS	yes	0	no	1	yes	Mongolian		CC	F			
31+	LS	no	0	no	1	no	Belgian	20	TT	M	CC	M	−20
32+	LS	yes	2	no	1	yes	Belgian	22	CC	M			
33+	LS	yes	2	yes	2	yes	Belgian	28	CT	M			
34+	LS	yes	2	yes	3	yes	Belgian		CT	F			
35+	S	yes	2	no	1	yes	Belgian	33	CT	M			
36+	LS	yes	2	no	3	yes	Belgian	27	CC	M			
37+	LS	yes	NA	yes	2	yes	Belgian	26	CT	F			
38+	LS	yes	2	yes	2	yes	Belgian		CT	F			
39+	LS	yes	2	yes	3	yes	Belgian	28	CT	F			
40+	LS	yes	2	no	1	yes	Belgian	32	CC	M			
41+	LS	no	NA	no	3	yes	Belgian	36	CC	M	CT	M	−26
42+	L	yes	2	yes	3	yes	Ukrainian	20	CC	F			
43+	LS	yes	2	no	1	yes	Belgian	25	CC	F	TT	M	20
44+	LS	yes	2	yes	3	yes	Belgian		CC	M			
45+	LS	yes	2	yes	3	yes	Belgian	29	CT	F			
46+	LS	yes	2	yes	3	yes	Belgian		CC	F			
47+	S	yes	2	no	1	yes	Moroccan	31	CT	F			
48+	LS	yes	2	yes	2	yes	Belgian	27	CT	F			
49+	S	yes	2	yes	3	yes	Belgian	34	CC	F			
50+	S	no	NA	no	1	yes	Belgian	36	CT	F	CC	F	17
51+	LS	yes	2	no	3	yes	Belgian	30	CC	F			
52+	LS	yes	2	no	1	yes	Moroccan	24	CC	F			
53+	S	yes	2	no	1	yes	Belgian	28	CC	F			
54+	S	no	NA	no	1	yes	Belgian		CT	F			
55+	LS	yes	2	no	2	yes	Bosnian	31	CT	F	CC	M	53
56+	S	no	0	no	1	yes	Belgian	30	CC	F			

(*Continued on next page*)

Table 1 Background information of MMC patients included in the HumanMethylation450 BeadChip and Sequenom EpiTYPER *(Continued)*

MMC patient	Type MMC	Hy/VP	ACM	Scoliosis	ADL	UI	Ethnicity	Maternal age (years) at birth of MMC patient	MMC patient		Sibling		MMC patient versus sibling age (months)
									MTHFR 677C>T	Gender	MTHFR 677C>T	Gender	
57+	LS	yes	2	no	1	yes	Belgian	24	CC	F			
58+	S	no	2	no		yes	Moroccan	26	CC	F			
59+	LS	yes	2	yes	3	yes	Belgian	27	CC	F			
60+	LS	yes	2	no	1	yes	Turkish	35	CT	F	CC	F	−101
61+	LS	yes	2	yes	3	yes	Belgian		CT	F			
62+	LS	yes	2	no	1	yes	Turkish	29	CT	F			
63+	LS	yes	2	yes	3	yes	Belgian	35	CT	F			
64+	L & CP	yes	2	no	2	yes	Belgian	40	CT	F	CT	F	−27
65+	LS	yes	2	yes	2	yes	Belgian		CT	F			
66+	LS	yes	2	yes	2	yes	Belgian	24	CT	F			
67+	LS	yes	2	yes	2	yes	Belgian		CT	F			
68+	S	yes	2	no	1	no	Belgian		CT	M			
69+	LS	yes	2	yes	3	yes	Belgian	24	CT	M			
70+	LS	yes	2	yes	3	yes	Belgian	29	CC	M			
71+	LS	yes	2	yes	3	yes	Belgian	33	CC	F			
72+	LS	yes	2	yes	2	yes	Belgian	29	CC	M			
73+	LS	yes	2	yes	3	yes	Belgian	29	CT	F	CT	F	−24
74+	LS	yes	2	yes	2	yes	Belgian		CT	M			
75+	LS	yes	2	no	1	yes	Belgian		CC	F			
76+	LS	yes	2	yes	2	yes	Belgian	31	CT	F			
77+	LS	yes	2	yes	3	yes	Belgian	26	CC	M			
78+	LS	yes	2	yes	3	yes	Belgian	30	CT	M			
79+	S	no	0	no	1	yes	Belgian		CT	M			
80+	LS	yes	2	no	1	yes	Belgian	30	CC	F			
81+	LS	yes	NA	no	2	yes	Turkish		CT	M			
82+	TL	yes	2	yes	3	yes	Belgian		TT	F			
83+	TL	yes	2	yes	1	yes	Belgian	24	TT	F			
84+	TL	yes	1	yes	3	yes	Belgian	37	CC	F			
85+	TL	yes	2	no	1	no	Belgian		TT	F			

*Inclusion in HumanMethylation 450K BeadChip (10 MMC patients) and +Sequenom EpiTYPER (83 MMC patients); MMC: myelomeningocele; M: male; F: female; S: Sacral; LS: Lumbosacral; TL: Thoracolumbal; CP: Cheilopalatoschisis; Hy/VP: presence of hydrocephaly and ventriculoperitoneal drain; ACM: Arnold Chiari Malformation: 1 = type 1, 2 = type 2; NA: Not Available; ADL: Activities of daily life: 1 = ambulatory, 2 = household ambulatory with wheelchair for longer distances, 3 = wheelchair dependent; UI: urinary incontinence; *MTHFR 677C>T* genotype (*CC/CT/TT*) in 85 MMC patients: 47% *CC* - 53% *CT/TT* vs. 40% *CC* - 60% *CT/TT* in 30 healthy unrelated controls (*P*-value = ns).

The methylation hypothesis suggests that folic acid prevents NTDs by enhancing cellular methylation reactions. It is known that a tight regulation of genome-wide erasure of epigenetic footprints with resetting of the methylation signature is critical for normal embryogenesis and, therefore, it is believed that DNA methylation changes and genomic instability may disturb neural tube folding. [13] Immediately post fertilization, rapid de-methylation takes place, followed by re-methylation in the blastocyst and early embryo. It is expected that changes in cytosine methylation are not randomly distributed in the genome but are preferentially located at loci that are more sensitive to these processes. Methylome analysis during early embryonic differentiation showed changes in the methylation patterns for developmental regulatory genes, such as Homeobox (*HOX*) genes. [14] The *HOX* gene clusters comprise a family of genes assembled in 4 clusters (*HOX A, B, C,* and *D*, located on chromosomes 7, 17, 12, and 2, respectively). *HOX* genes encode highly conserved transcription factors expressed in the brain and spinal cord that play a central role in establishing the anterior-posterior body axis during embryogenesis (**Fig. S1**). [15,16] Their expression is tightly regulated in a spatio-temporal and collinear manner, partly by chromatin structure and epigenetic modifications. [17-19] Though genetic studies could not show an association between variants in *HOX* genes and NTDs,[15] DNA methylation studies for the *HOX* cluster genes have not yet been performed.

We hypothesize that children born from mothers with folic acid resistance and a disturbed methylation cycle can present with an abnormal DNA methylation profile for *HOX* genes, resulting in increased risk for abnormal embryonic development and NTDs. Therefore, the aim of this study was to investigate DNA methylation of *HOX* genes as mediator of NTD risk using data extracted from a genome-wide DNA methylation analysis study performed for 10 patients with lumbosacral MMC and 6 healthy unrelated controls. A validation study was performed to quantify locus-specific methylation differences in larger cohorts. The functional

Table 2 Methylation of the *HOX* genes using the HumanMethylation450 BeadChip and analysis

Cluster	Gene	Chr	Illumina ID	*P*-value <0.05	β-diff >0.05	Ctrls (n = 6)		MMC (n = 10)	
						Mean	SD	Mean	SD
A: Chr.7p14	*HOXA2*	7	cg06055873	0.016	−0.06	0.32	0.03	0.26	0.04
	HOXA2	7	cg19432993	0.031	−0.12	0.69	0.05	0.57	0.12
	HOXA2	7	cg06166490	0.016	−0.12	0.70	0.06	0.58	0.11
	HOXA2	7	cg04027736	0.022	−0.11	0.61	0.06	0.50	0.11
	HOXA2	7	cg00445443	0.042	−0.10	0.41	0.08	0.31	0.11
		7	cg15037137	0.007	−0.05	0.85	0.02	0.80	0.07
	HOXA4	7	cg25952581	0.042	−0.09	0.45	0.06	0.37	0.11
	HOXA4	7	cg17591595	0.042	−0.08	0.73	0.05	0.65	0.09
	HOXA11	7	cg24709033	0.011	−0.06	0.27	0.03	0.21	0.04
B: Chr.17q21	*HOXB5*	17	cg01405107	0.042	0.09	0.49	0.05	0.58	0.08
	HOXB6	17	cg09983216	0.016	−0.13	0.55	0.08	0.42	0.10
	HOXB7	17	cg11041817	0.007	−0.29	0.70	0.08	0.41	0.20
	HOXB7	17	cg22622477	0.007	−0.16	0.36	0.06	0.20	0.09
	HOXB7	17	cg07547765	0.007	−0.26	0.71	0.10	0.44	0.18
		17	cg19051015	0.022	−0.09	0.72	0.05	0.63	0.07
	HOXB9	17	cg15117739	0.007	−0.10	0.68	0.04	0.57	0.07
	HOXB9	17	cg12057127	0.042	−0.06	0.72	0.01	0.67	0.07
		17	cg20454400	0.031	−0.06	0.37	0.04	0.31	0.05
		17	cg16654603	0.011	−0.09	0.67	0.02	0.58	0.08
		17	cg02052915	0.016	−0.05	0.36	0.03	0.31	0.04
C: Chr.12q13		12	cg08299265	0.016	−0.06	0.39	0.04	0.33	0.03
		12	cg26643142	0.031	−0.06	0.35	0.03	0.30	0.05
	HOXC4	12	cg18473521	0.011	−0.12	0.43	0.08	0.31	0.07
D: Chr.2q31	*HOXD9*	2	cg04730882	0.005	−0.07	0.35	0.03	0.28	0.05
		2	cg07783843	0.011	−0.06	0.24	0.02	0.18	0.04
		2	cg05525812	0.007	−0.07	0.25	0.02	0.18	0.05

Nucleotide positions in accord to NCBI build 37/hg19. Selection is performed along both β-value > 0.05 difference and *P*-value < 0.05; calculated with Wilcoxon Rank-Sum test. The 3 probes in **bold** are located within the same CpG island at Chr17:46,685,244–46,685,449 within the *HOXB7* gene body. This region was selected for the validation study using Sequenom EpiTYPER. β-diff: β-difference; Chr: chromosome; Ctrls: controls; MMC: myelomeningocele.

characterization of the candidate *HOX* gene was finally analyzed using a zebrafish model of neural tube formation.

Results

DNA methylation analysis of the different *HOX* genes in MMC case-control study

Methylation values for all CpGs located within the 4 *HOX* clusters were extracted from data obtained from a 450K array-based genome-wide methylation analysis, using leukocyte DNA from 10 MMC cases and 6 unrelated age- and gender-matched healthy controls. Detailed clinical characteristics of these MMC patients are reported in **Table 1**. Pie charts were made to show the equal distribution of the filtered CpG probes (n = 967) based on: i) location within the 4 different *HOX* clusters; ii) location with respect to gene transcripts; and iii) location with respect to the CpG island (**Fig. S2**). From the 967 filtered CpGs profiled on the 450K array (**Table S1**), only 26 CpGs were found to be differentially methylated between MMC patients and controls (**Table 2**, **Fig. S2**). Interestingly, 25 of these 26 CpGs were hypomethylated for the MMC patients and 20 of the 26 CpGs were located within the *HOXA* or *HOXB* clusters. Only for the *HOXB7* gene, 3 different CpG probes (cg11041817, cg22622477, and cg07547765) were significantly hypomethylated in MMC patients (β-differences of −0.29, −0.16, and −0.26, respectively, with all *P*-values of 0.007). These 3 probes are located within a single CpG island at chr17:46,685,244–46,685,449, within the *HOXB7* gene body (**Fig. 1A**).

HOXB7 methylation analysis in MMC case-control study

A validation study using larger cohorts (83 MMC patients described in **Table 1**) was performed with the Sequenom EpiTYPER technology to quantify methylation of the above selected CpG islands located in the *HOXB7* gene body. A Sequenom amplicon was developed that covers 26 CpGs (**Fig. 1A**), including the 3 significant CpGs detected in the 450K array. Within this amplicon, the EpiTYPER detected 10 analytical CpG units for which CpG6 is similar to cg07547765. DNA methylation values for the amplicon for 83 MMC patients and 30 unrelated healthy controls were normally distributed (Shapiro-Wilk test, P>0.05). A significant *HOXB7* hypomethylation (*P*-value < 0.0001) was detected for MMC patients versus controls with mean methylation values of 41% (95% CI: 38–45%) vs. 56% (95% CI: 50–61%), respectively (**Fig. 1B**). The mean level of methylation for each CpG unit within the amplicon was also significantly different between MMC patients and controls (**Fig. 1C** and **Table S2**). To exclude an effect of changes in methylation

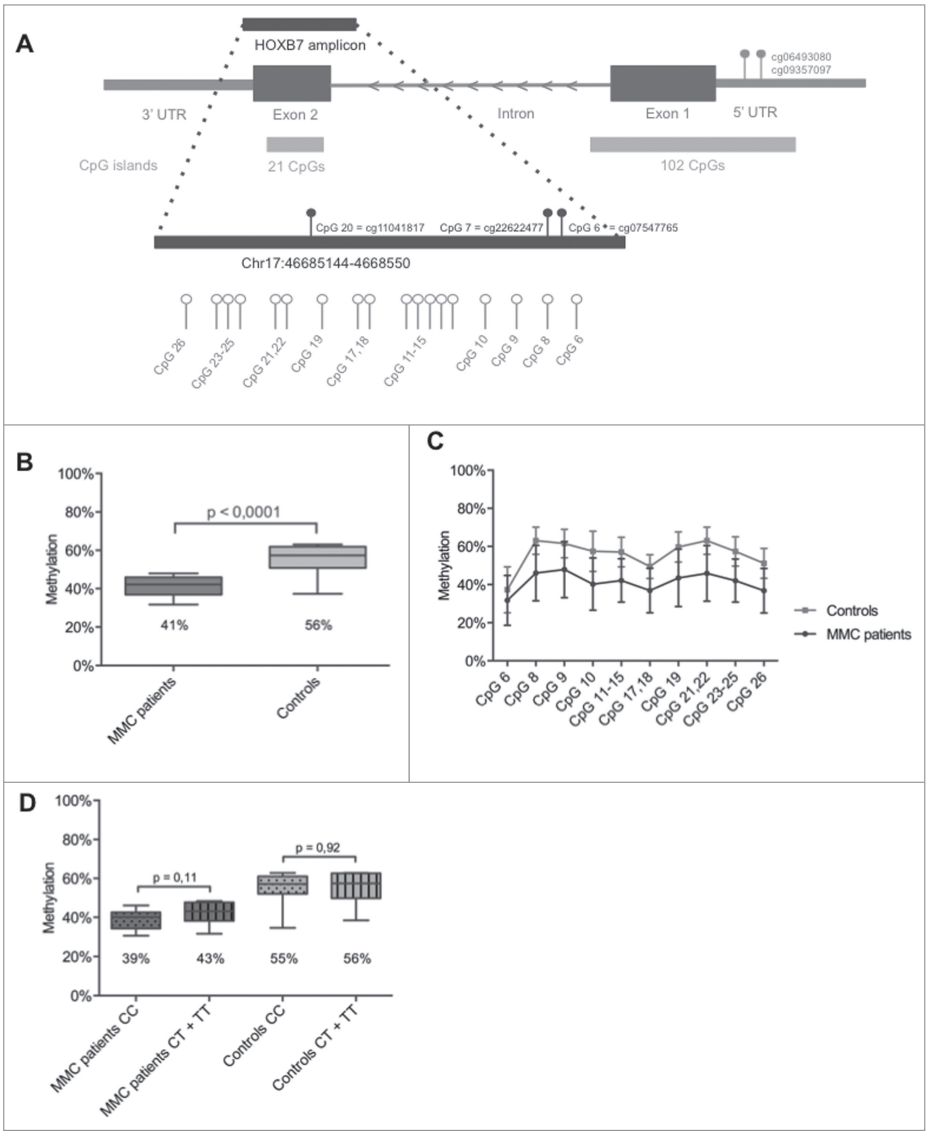

Figure 1. HOXB7 methylation studies by Sequenom EpiTYPER in MMC patients. A: Localization of the studied amplicon (Chr17:46,685,144–46,685,550) within *HOXB7* Exon 2. The amplicon covers 26 single CpGs and our assay provides data 10 analytical CpG units. Nucleotide positions accord to the NCBI build 37/hg19. The CpG units studied by 450K Array (cg11041817, cg22622477 and cg07547765) and the *in silico* analysis (cg06493080, cg09357097) are also indicated. **B**: Boxplot representing the methylation pattern of MMC patients and controls with box = 25th and 75th percentiles; bars = min and max values. The mean methylation level of each group is shown below the plot. **C**: Methylation pattern for each CpG unit within the amplicon. Wilcoxon Rank-Sum test was performed. **D**: Boxplot representing the methylation pattern of MMC patients and controls divided according to *MTHFR 677C>T* genotype with box = 25th and 75th percentiles; bars = min and max values. The mean methylation level of each group is shown below the plot.

due to differences in ethnicity, the *HOXB7* methylation pattern between 70 Belgian MMC patients was compared to 10 non-Caucasian MMC patients without significant differences (**Fig. S3**).

As findings of global DNA hypomethylation and LINE-1 hypomethylation suggest that disruption of genomic stability may disrupt neural tube closure and the *MTHFR 677C>T* variant is associated with global DNA hypomethylation, we determined the *MTHFR 677C>T* variant for MMC patients and healthy controls (**Table 1**). Interestingly, an intrinsic defect in the folic acid pathway related to *MTHFR* activity seems not to be involved, as no association was found between *MTHFR 677 CC* versus *CT+TT* carriers and *HOXB7* methylation (**Fig. 1D**).

HOXB7 methylation analysis in unaffected siblings of MMC patients

For 12 out of 83 MMC patients, DNA was also collected from their healthy siblings (**Table 1**). Remarkably, the mean methylation level of the *HOXB7* amplicon was not different between MMC patients and their unaffected siblings with values of 37% (95% CI: 33–40%) vs. 40% (95% CI: 37–42%) (**Fig. 2A**). Multiple T-testing for each CpG within the *HOXB7* amplicon also showed no significant differences between patients and healthy siblings (**Fig. 2B** and **Table S2**).

HOXB7 methylation versus expression

Since leukocyte RNA was not collected for our cohorts, we used the MENT database to estimate a correlation between *HOXB7* methylation and gene expression. The 2 CpGs (cg09357097 and cg06493080) located in the *HOXB7* promoter (**Fig. 1A**) showed no correlation with gene expression in normal brain and blood tissues. However, there is evidence that lower *HOXB7* methylation values in brain tightly regulate higher and stable gene expression levels compared to the higher methylation levels in blood that are associated with variable gene expression (**Fig. S4**). Interestingly, cg06493080 showed strong negative correlation with gene expression in different cancer tissues, especially for brain (correlation −0.15; *P*-value = 0.008).

Hoxb7a overexpression and depletion in zebrafish

Functional genetics was performed in zebrafish to study alterations in Hoxb7a expression during embryogenesis and neural tube formation. The regulation of the *HOX* clusters is highly conserved between humans and zebrafish (**Fig. S1**). Hoxb7a has an anterior expression limit adjacent to the somite 3–4 boundary at the 20 somite stage. [20] We analyzed embryos with Hoxb7a

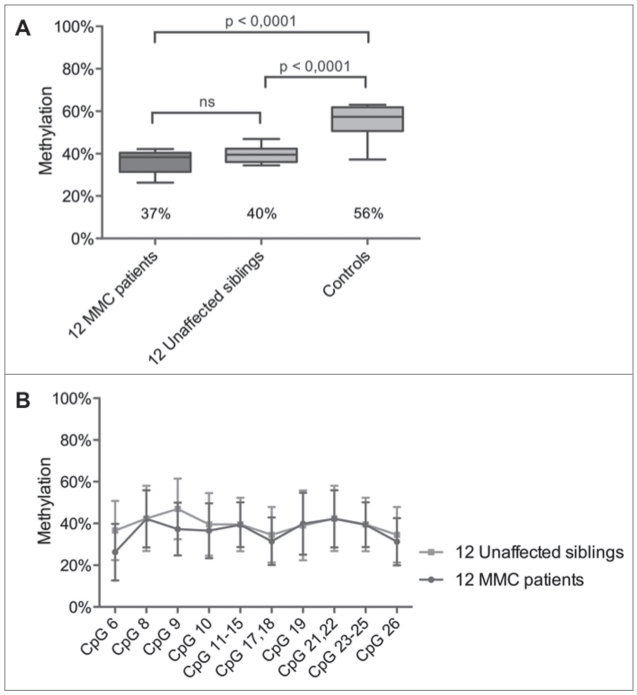

Figure 2. *HOXB7* methylation studies by Sequenom EpiTYPER in pairs of unaffected siblings vs. MMC patients. A: Boxplot representing the methylation pattern of affected siblings and unaffected siblings with box = 25th and 75th percentiles; bars = min and max values. The mean methylation level of each group is shown below the plot. **B**: Methylation pattern for each CpG unit within the amplicon. Wilcoxon Rank-Sum test was performed.

depletion and overexpression using microinjection of a splice morpholino (MO) and synthetic Hoxb7a mRNA, respectively. MO-induced Hoxb7a depletion resulted in hypopigmentation and developmental delay with dysmorphy in 83–94% of the embryos at 24 hours post fertilization (hpf) (**Fig. S5**). However, pax2a staining to visualize neural tube formation at 24 hpf was not different between Hoxb7a- or control-MO injected embryos, even for the severely affected Hoxb7a depleted embryos (**Fig. S5**). Embryos injected with different concentrations of Hoxb7a mRNA also presented with severe to mild malformations in about 48–71% of the embryos at 24 hpf (**Fig. 3B**). These embryos had shorter anterior/posterior axes as well as crooked or bent tails (**Fig. 3A**). Interestingly, pax2a staining after overexpression of Hoxb7a for different concentrations showed a neural tube was that was absent or completely disorganized (**Fig. 3C**).

Discussion

As *HOX* genes play key roles in neural tube closure and many studies have shown that folic acid prevents NTDs by stimulating cellular methylation reactions, we extracted methylation data for the different *HOX* genes from a genome-wide DNA methylation analysis performed for 10 MMC patients and 6 unrelated healthy controls. Interestingly, 25 of the 26 CpGs were hypomethylated for the MMC patients with the *HOXB7* gene body as most significant locus. Interestingly, *HOXB7* hypomethylation was not only confirmed in a larger MMC cohort but was also detected in 12 healthy siblings each related to a MMC patient. These results are suggestive of a maternal effect that contributes to *HOXB7* hypomethylation. Additional healthy siblings must be recruited but gender, age, *MTHFR 677C>T* genotype, or whether MMC is the firstborn, did not seem to be predictive risk factors for NTDs, based on data for these sibling pairs (**Table 1**). *HOXB7* hypomethylation by itself is not likely to be causative for NTDs but rather be part of a complex combination of environmental and (epi)genetic risk factors. We found no association between *MTHFR CC* vs. *CT+TT* carriers and *HOXB7* methylation, suggesting that an intrinsic defect in the folic acid pathway related to *MTHFR* activity is not involved. Though we made no measurements of maternal folic acid levels or uptake, it is known that folic acid levels in most affected pregnancies are within the normal range, [7] and, despite optimal supplementation, a significant proportion of NTDs are unresponsive to folic acid. [6,8] We therefore hypothesize that these mothers have folic acid resistance leading to a disturbed methylation cycle with alterations in DNA methylation and an increased risk for abnormal embryonic development. Additional studies must be undertaken to study the association between maternal folic acid intake and *HOXB7* methylation in DNA from the mother and her offspring.

HOX genes encode for evolutionary highly conserved transcription factors expressed in the central nervous system (**Fig. S1**). They are tightly regulated in a spatiotemporal and collinear manner [17-19], patterning the embryo along the rostro-caudal axis. The *HOXA* and *HOXB* clusters have a closer phylogenetic relationship and hence share more functionality than with either the *HOXC* or *HOXD* cluster. [21] Their cooperative functioning is necessary for the generation of the cranial neural crest and craniofacial diversity. [22-24] The spinal cord is a caudal structure, but the neural cells from which it derives initially express rostral, forebrain-like characteristics. The caudal character emerges soon after neural induction, through different extrinsic signals. [25,26] According to our study, differential *HOX* gene methylation in MMC patients occurs in both anterior and posterior *HOX* genes. Moreover, failure in establishing correct *HOX* gene methylation in the *HOXA* and *HOXB* clusters may result in disturbances in neural cell identity that ultimately leads to neural malformations. *HOX* gene clusters are evolutionary highly conserved between human and zebrafish and a neural tube formation zebrafish model was previously used to study *VANGL1*. [27] HOX7 has 2 paralog members in humans and only one in zebrafish (**Fig. S1**) but the zebrafish Hoxb7a gene shares 60% homology with the human *HOXB7* sequence. As *HOXB7* hypomethylation is suggestive for *HOXB7* overexpression, Hoxb7a overexpression experiments were performed in zebrafish. Overexpression of Hoxb7a in zebrafish resulted in developmental abnormalities and pax2a staining showed abnormal neural tube formation in about 60% of the embryos.

In the present study, we were not able to use patient DNA samples from brain or spinal cord tissue. Concordant DNA

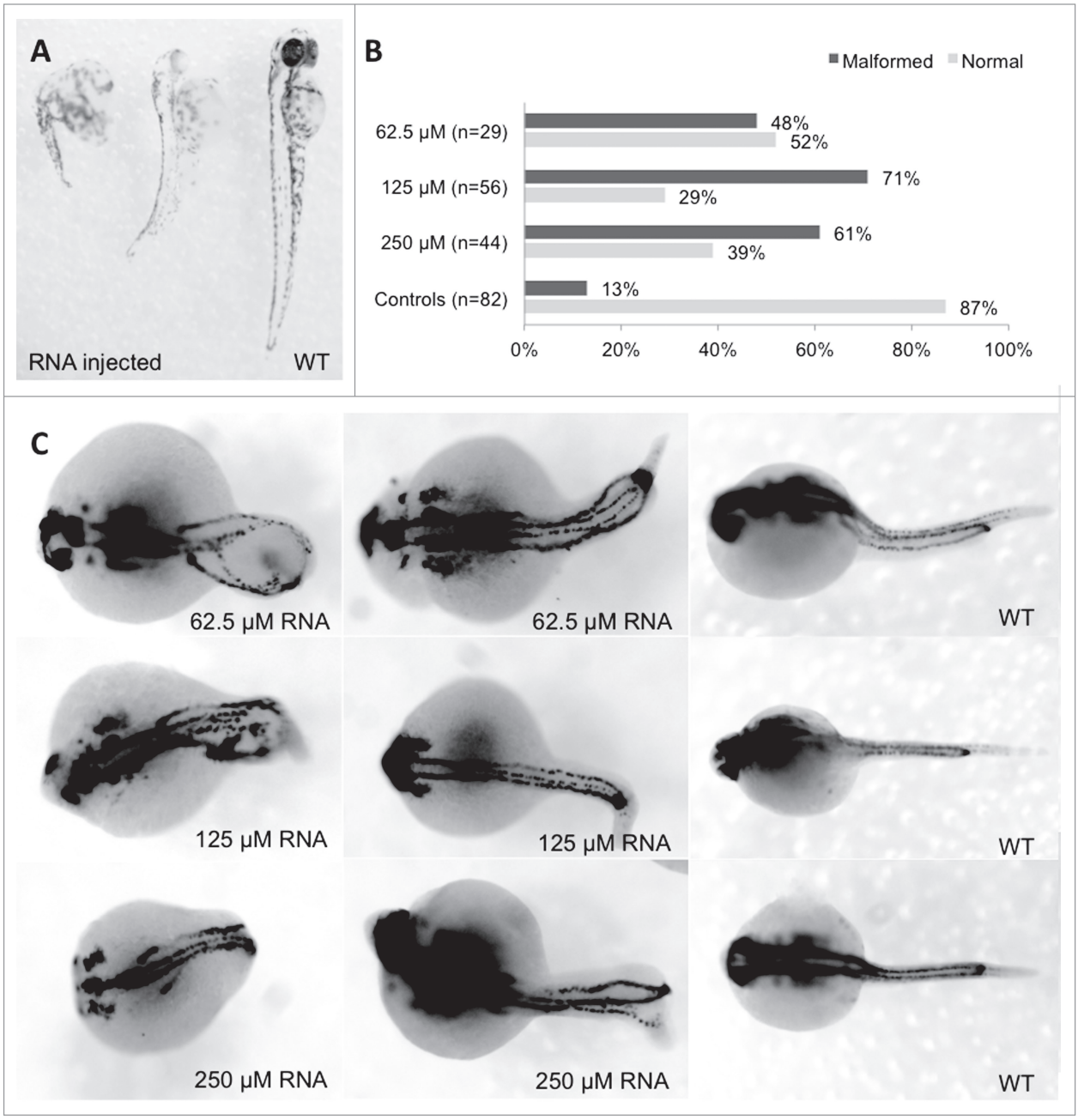

Figure 3. Phenotype analysis of Hoxb7a-overexpression in zebrafish embryos. A: Phenotype analysis at 72 hpf of Hoxb7a mRNA injected zebrafish resulted in significant hypopigmentation and malformation in 66% of the injected zebrafish. These embryos had shorter anterior/posterior axes as well as crooked or bent tails. **B**: Phenotype analysis after pax2a at 24 hpf resulted in about 63% embryos with a mild or severe affected phenotype after Hoxb7a overexpression compared to 13% in injected controls. **C**: Pax2a staining after microinjection of different concentrations of mRNA. From left to right severe, mild affected and wild type (WT) embryos at 24 hpf. WT zebrafish show expression in the hindbrain, hindbrain-midbrain boundary, neural tube, mesoderm, optic stalk, otic vesicle, and pronephric duct. Microinjection 62.5 µM mRNA, 125 µM mRNA and 250 µM mRNA resulted in respectively 48%, 71% and 61% malformed zebrafish. There was no correlation between mRNA dosage and severity of malformation.

methylation profiles in brain and blood samples from the same individuals suggest that blood might hold promise as surrogate for brain tissue to detect DNA methylation. [28-30] Genome-wide methylation arrays revealed similar methylation patterns for the *HOX* genes in breast cancers and white blood cells, which suggests that methylation is more likely to be a normal developmental and tissue-specific process that does not directly relate to the malignant mechanism. [31] Interestingly, functional *in silico* analysis using the MENT database showed no correlation with gene expression in normal brain and blood tissues for the methylation of 2 *HOXB7* promoter CpGs but there is evidence that lower *HOXB7* methylation values in brain tightly regulate

higher and stable gene expression levels compared to the higher methylation levels in blood that are associated with a variable *HOXB7* gene expression. These data would suggest that *HOXB7* hypomethylation is associated with higher gene expression. A limitation of our study was the lack of *HOXB7* gene expression studies using leukocyte RNA from MMC cases and unrelated healthy controls as RNA samples were not collected. Additional studies are needed to correlate the methylation levels of the *HOXB7* gene body CpGs with *HOXB7* gene or protein expression values. Furthermore, it would be interesting to compare our findings in leukocytes with those from neural tissue.

Conclusion

This is the first study that uses genome-wide DNA methylation data for the locus-specific analysis of the different *HOX* genes in patients with NTDs. We found evidence that *HOXB7* hypomethylation is a potential risk factor for MMC but also that the underlying methylation defect is present in both affected and non-affected offspring. This could confirm the hypothesis that children born from mothers with folic acid resistance and a disturbed methylation cycle, can present with alterations in DNA methylation with high risk for abnormal embryonic development. Investigating the complex etiology of NTDs requires consideration of more DNA methylation studies; therefore, genome-wide DNA methylation analysis without focusing on candidate pathways could reveal more epigenomic changes associated with NTDs. The challenge ahead is to determine which DNA regions are more sensitive to methylation changes during embryogenesis and lead to NTDs.

Materials and Methods

Ethics statement

Written informed consent to collect blood samples for (epi) genetic studies was obtained from all participants and/or their legal representatives. This study was approved by the Medical Ethics Committee of the University of Leuven (study ML9193).

Description of MMC patients, related healthy siblings and unrelated healthy controls

A total of 85 MMC patients and 12 healthy related siblings enrolled in this study are followed at the pediatric neurology department of the University Hospital Leuven (all <18 y old). Detailed clinical and general characteristics for all these subjects are reported in **Table 1**. As sensory and motor functions at and below the level of the spinal cord defect are impaired, paralysis, bowel, and bladder dysfunction is present in most of the patients. Folic acid supplementation was recommended, but red blood cell folate was not measured during pregnancy. **Table 1** also indicates which MMC patients were included in the 450K array and/or the Sequenom validation study. In addition, we have recruited 30 age- and gender-matched non-related healthy control subjects with no family history of NTDs (15 males and 15 females).

Genome-wide DNA methylation analysis using the Illumina 450K BeadChip array

Genome-wide DNA methylation analysis was assessed using Illumina Infinium HumanMethylation450 BeadChip (Illumina, Inc., California, USA) that provides a genome-wide coverage of CpG sites (99% of RefSeq genes, covering the promoter region, 5′UTR, first exon, gene body and 3′UTR; **Figure S1A**). [32] Bisulfite conversion of leukocyte DNA (1 μg) was performed using the EZ DNA methylation kit (Zymo Research, Irvine CA, USA). Control nested PCR reactions were done on both unconverted and converted DNA to verify DNA conversion. Arrays were processed according to the manufacturer's protocol. Samples were randomly distributed to control for batch effects. Before analyzing the data, possible sources of technical bias were excluded. Probes were excluded from further analysis if >95% of samples had a detection value >0.01. [33] The software GenomeStudio (Illumina) was used to convert on-chip fluorescent methylation values into numerical values (β-value). Methylation, described as a β-value, is a continuous variable ranging between 0 (no methylation) and 1 (full methylation) for each CpG site. From this genome-wide analysis, we extracted the methylation levels for the different CpGs that cover all regions within the *HOX* clusters (for overview see **Table S1**). We discarded the following probes (608 in total): i) probes with absent signals in one or more of the DNA samples analyzed; ii) non-CpG probes; iii) probes containing SNPs; and iv) leukocyte-specific probes. [33] The signal processing was conducted using the Illumina Methylation Analyzer (IMA) package implicated in the open source statistical environment R. [34] Two filters were applied to identify differentially methylated CpGs between MMC patients and controls: i) absolute β-value difference > 0.05 and ii) *P*-value < 0.05, as calculated with the Wilcoxon rank-sum test.

Methylation of CpGs within the *HOXB7* gene body using the Sequenom EpiTYPER

Leukocyte DNA (1 μg) was subjected to bisulfite treatment using the MethylDetector™ bisulfite modification kit (Active Motif, Carlsbad CA, USA) as we described. [35,36] The Sequenom MassARRAY (Sequenom, San Diego, CA, USA) was used for quantitative DNA methylation analysis of the CpG island within the *HOXB7* gene body using conditions described. [35] Long cycling incubation was applied to further optimize the conversion reaction. [37] Primers were designed using the Sequenom EpiDesigner BETA software (www.epidesigner.com), taking into account amplicon coverage, number of CpGs, fragment size and number of nucleotide repeats in the primer sequence. The primers were: 5′-aggaagagagGTGTTGGGATTATAGGTTTGAGTTT-3′ and 5′-cagtaatacgactcactatagggagaaggctACTAAACTTCTCTTCCTCTCCCTTTC-3′. This 395 bp long amplicon covers 26 CpGs but the EpiTYPER analysis only detected 10 separate analytical units that comprise single, duplicate or triplicate CpGs as shown in **Figure 1A**. The Illumina probe cg07547765 is similar as CpG6. The 2 other Illumina probes cg11041817 and cg22622477 are located within the studied CpG Sequenom amplicon but were not detected by the EpiTYPER. PCR steps were performed in

triplicate for each DNA sample and a standard deviation between replicates was mostly <10%. When triplicate measurements had a SD > 10% or when only one of the triplicates was available, data for that sample were excluded. The mean of 3 values was used for further analyses. The EpiTYPER analysis method reports CpG methylation values as percentage. Statistical analyses to quantify DNA methylation differences were performed using the Prism 6 software (GraphPad Software Inc., San Diego, CA, USA). A two-tailed T-test was used to assess differences in mean DNA methylation levels between cohorts for the overall *HOXB7* amplicon considered as methylation average and for each CpG unit within this amplicon separately.

MTHRF 677C>T genotyping

Leukocyte DNA from MMC patients, related healthy siblings and unrelated healthy controls was screened for the presence of the *MTHFR 677C>T* variant by PCR and restriction digestion as described. [38]

Functional *in silico* analysis of *HOXB7* methylation versus expression

A correlation between *HOXB7* CpG promoter methylation and gene expression was studied by data mining using the open source database MENT (Methylation and Expression database of Normal and Tumor tissues). [39] The database only included Illumina 27K BeadChip CpG probes (cg09357097 and cg06493080, as shown in **Fig. 1A**) that are located in the *HOXB7* promoter and not in the gene body.

Hoxb7a overexpression and depletion in zebrafish

Wild-type AB zebrafish strains were maintained according to standard protocols. [40] Embryos were produced by natural mating and collected and fixed at different stages based on standard morphological criteria. [41] To produce Hoxb7a mRNA, the full coding Hoxb7a transcript (NM_001115091.2) was PCR amplified and cloned in the pGEM T Easy vector (Promega, Madison, WI, USA). Forward and reverse primers were 5′-ATGAGTTCATTGTATTATGCGA-3′ and 5′-GTAGTTTATACATCTATATTAA-3′. Next, capped and polyadenylated Hoxb7a mRNAs were synthesized using mMESSAGE mMACHINE® High Yield Capped RNA Transcription Kit and Poly(A) Tailing Kit (both from Ambion, Austin, TX, USA) according to the manufacturer's protocol. The synthesized mRNA was diluted in phenol red to different concentrations as indicated in the figure legends. Morpholino (MO) injection was performed with a splice Hoxb7a-MO (5′-AGCACCTGTGAAAAGCGCAGAATGA-3′). This MO was designed against Chr17: 46,685,144–46,685,550. Off-target effects were assessed by injecting with a standard control MO against β-globin (5′-CCTCTTACCTCAGTTACAATTTATA 3′). MOs were designed by Gene Tools, LLC (Philomath, OR, USA). All injected embryos were life-screened at 24, 48, and 72 hours post-fertilization (hpf) using a Zeiss Lumar V12 (Carl Zeiss Microscopy, Thornwood, NY, USA) and images were captured with a Leica DFC310 FX digital color camera (Leica Microsystems, Wetzlar, Germany). Overexpression and depletion experiments were performed in duplicate. Ethical approval was obtained for these studies.

Pax2a whole mount in situ hybridization

Whole mount In Situ Hybridization (WISH) with a probe for the paired box gene 2a (pax2a) was performed 24 hours after injection of MOs or Hoxb7a mRNA. Pax2a cDNA obtained from Dr. W. Driever (University of Freiburg, Germany) was cloned in the pGEM-3zf+ for the synthesis of a digoxigenin (DIG) labeled antisense RNA probe as described. [42] The Pax2a probe was subsequently used to analyze the influence of Hoxb7a overexpression and inhibition on spinal cord and notochord formation using standard morphological criteria. [41] WISH experiments were performed in duplicate. Embryos were screened using a Zeiss Lumar V12 (Carl Zeiss Microscopy, Thornwood, NY, USA) and images were captured with a Leica DFC310 FX digital color camera (Leica Microsystems, Wetzlar, Germany).

Disclosure of Potential Conflicts of Interest

No potential conflicts of interest were disclosed.

Acknowledgments

This work was supported by the Fund for Scientific Research-Flanders (FWO-Vlaanderen, Belgium) [G.0A23.14N and G.0B17.13N; 12M2715N to BI] and by the Research Council of the University of Leuven (Onderzoeksraad KU Leuven Belgium) [OT/14/098]. CVG is holder of the Bayer and Norbert Heimburger (CSL Behring) Chairs and is holder of a clinical-fundamental research mandate of the Fund for Scientific Research-Flanders.

Supplemental Material

Supplemental data for this article can be accessed on the publisher's website.

References

1. Wallingford JB, Niswander LA, Shaw GM, Finnell RH. The continuing challenge of understanding, preventing, and treating neural tube defects. Science 2013; 339:1222002; PMID:23449594; http://dx.doi.org/10.1126/science.1222002
2. Copp AJ, Stanier P, Greene ND. Neural tube defects: recent advances, unsolved questions, and controversies. Lancet Neurol 2013; PMID:23790957
3. Au KS, Ashley-Koch A, Northrup H. Epidemiologic and genetic aspects of spina bifida and other neural tube defects. Dev Disabil Res Rev 2010; 16:6-15; PMID:20419766; http://dx.doi.org/10.1002/ddrr.93
4. Harris MJ, Juriloff DM. Mouse mutants with neural tube closure defects and their role in understanding human neural tube defects. Birth Defects Res A Clin Mol Teratol 2007; 79:187-210; PMID:17177317; http://dx.doi.org/10.1002/bdra.20333
5. Harris MJ, Juriloff DM. An update to the list of mouse mutants with neural tube closure defects and advances toward a complete genetic perspective of neural tube closure. Birth Defects Res A Clin Mol Teratol 2010; 88:653-69; PMID:20740593; http://dx.doi.org/10.1002/bdra.20676
6. Blom HJ, Shaw GM, den Heijer M, Finnell RH. Neural tube defects and folate: case far from closed. Nat Rev Neurosci 2006; 7:724-31; PMID:16924261; http://dx.doi.org/10.1038/nrn1986
7. Kirke PN, Molloy AM, Daly LE, Burke H, Weir DG, Scott JM. Maternal plasma folate and vitamin B12 are independent risk factors for neural tube defects. QJ Med 1993; 86:703-8; PMID:8265769

8. Cavalli P, Copp AJ. Inositol and folate resistant neural tube defects. J Med Gen 2002; 39:E5; PMID:11836374
9. Chen X, Guo J, Lei Y, Zou J, Lu X, Bao Y, Wu L, Wu J, Zheng X, Shen Y, et al. Global DNA hypomethylation is associated with NTD-affected pregnancy: A case-control study. Birth Defects Res A Clin Mol Teratol 2010; 88:575-81; PMID:20641100; http://dx.doi.org/10.1002/bdra.20670
10. Friso S, Choi SW, Girelli D, Mason JB, Dolnikowski GG, Bagley PJ, Olivieri O, Jacques PF, Rosenberg IH, Corrocher R, et al. A common mutation in the 5,10-methylenetetrahydrofolate reductase gene affects genomic DNA methylation through an interaction with folate status. Proc Nat Acad Sci U S A 2002; 99:5606-11; PMID:11929966
11. Wang L, Wang F, Guan J, Le J, Wu L, Zou J, Zhao H, Pei L, Zheng X, Zhang T. Relation between hypomethylation of long interspersed nucleotide elements and risk of neural tube defects. Am J Clin Nutrit 2010; 91:1359-67; PMID:20164316; http://dx.doi.org/10.3945/ajcn.2009.28858
12. Chang H, Zhang T, Zhang Z, Bao R, Fu C, Wang Z, Bao Y, Li Y, Wu L, Zheng X, et al. Tissue-specific distribution of aberrant DNA methylation associated with maternal low-folate status in human neural tube defects. J Nutrit Biochem 2011; 22:1172-7; PMID:21333513; http://dx.doi.org/10.1016/j.jnutbio.2010.10.003
13. Greene NDE, Stanier P, Moore GE. The emerging role of epigenetic mechanisms in the aetiology of neural tube defects. Epigenetics 2011; 6:875-83; PMID:21613818; http://dx.doi.org/10.4161/epi.6.7.16400
14. Laurent L, Wong E, Li G, Huynh T, Tsirigos A, Ong CT, Low HM, Kin Sung KW, Rigoutsos I, Loring J, et al. Dynamic changes in the human methylome during differentiation. Genome research 2010; 20:320-31; PMID:20133333; http://dx.doi.org/10.1101/gr.101907.109
15. Volcik KA, Blanton SH, Kruzel MC, Townsend IT, Tyerman GH, Mier RJ, Northrup H. Testing for genetic associations in a spina bifida population: analysis of the HOX gene family and human candidate gene regions implicated by mouse models of neural tube defects. A J Med Genet 2002; 110:203-7; PMID:12116226; http://dx.doi.org/10.1002/ajmg.10435
16. Carpenter EM. Hox genes and spinal cord development. Dev Neurosci 2002; 24:24-34; PMID:12145408
17. Barber BA, Rastegar M. Epigenetic control of Hox genes during neurogenesis, development, and disease. Ann Anat 2010; 192:261-74; PMID:20739155
18. Chambeyron S, Bickmore WA. Chromatin decondensation and nuclear reorganization of the HoxB locus upon induction of transcription. GenDev 2004; 18:1119-30; PMID:15155579; http://dx.doi.org/10.1101/gad.292104
19. Boudadi E, Stower H, Halsall JA, Rutledge CE, Leeb M, Wutz A, O'Neill LP, Nightingale KP, Turner BM. The histone deacetylase inhibitor sodium valproate causes limited transcriptional change in mouse embryonic stem cells but selectively overrides Polycomb-mediated Hoxb silencing. Epigenet Chromat 2013; 6:11; PMID:23634885; http://dx.doi.org/10.1186/1756-8935-6-11
20. Prince VE, Joly L, Ekker M, Ho RK. Zebrafish hox genes: genomic organization and modified colinear expression patterns in the trunk. Development 1998; 125:407-20; PMID:9425136
21. Prince V. The hox paradox: more complex(es) than imagined. Dev Bio 2002; 249:1-15; PMID:12217314; http://dx.doi.org/10.1006/dbio.2002.0745
22. Philippidou P, Dasen JS. Hox genes: choreographers in neural development, architects of circuit organization. Neuron 2013; 80:12-34; PMID:24094100; http://dx.doi.org/10.1016/j.neuron.2013.09.020
23. Soshnikova N, Dewaele R, Janvier P, Krumlauf R, Duboule D. Duplications of hox gene clusters and the emergence of vertebrates. Dev Biol 2013; 378:194-9; PMID:23501471; http://dx.doi.org/10.1016/j.ydbio.2013.03.004
24. Vieux-Rochas M, Mascrez B, Krumlauf R, Duboule D. Combined function of HoxA and HoxB clusters in neural crest cells. Dev Biol 2013; 382:293-301; PMID:23850771; http://dx.doi.org/10.1016/j.ydbio.2013.06.027
25. Jessell TM. Neuronal specification in the spinal cord: inductive signals and transcriptional codes. Nat Rev Genet 2000; 1:20-9; PMID:11262869; http://dx.doi.org/10.1038/35049541
26. Doniach T. Basic FGF as an inducer of anteroposterior neural pattern. Cell 1995; 83:1067-70; PMID:8548794
27. Reynolds A, McDearmid JR, Lachance S, De Marco P, Merello E, Capra V, Gros P, Drapeau P, Kibar Z. VANGL1 rare variants associated with neural tube defects affect convergent extension in zebrafish. Mech Dev 2010; 127:385-92; PMID:20043994; http://dx.doi.org/10.1016/j.mod.2009.12.002
28. Masliah E, Dumaop W, Galasko D, Desplats P. Distinctive patterns of DNA methylation associated with Parkinson disease: identification of concordant epigenetic changes in brain and peripheral blood leukocytes. Epigenetics 2013; 8:1030-8; PMID:23907097; http://dx.doi.org/10.4161/epi.25865
29. Tylee DS, Kawaguchi DM, Glatt SJ. On the outside, looking in: a review and evaluation of the comparability of blood and brain "-omes". Am J Med Genet B Neuropsychiatr Genet 2013; 162B:595-603; PMID:24132893
30. Ikegame T, Bundo M, Murata Y, Kasai K, Kato T, Iwamoto K. DNA methylation of the BDNF gene and its relevance to psychiatric disorders. J Hum Genet 2013; 58:434-8; PMID:23739121; http://dx.doi.org/10.1038/jhg.2013.65
31. Avraham A, Sandbank J, Yarom N, Shalom A, Karni T, Pappo I, Sella A, Fich A, Walfisch S, Gheber L, et al. A similar cell-specific pattern of HOXA methylation in normal and in cancer tissues. Epigenetics 2010; 5:41-6; PMID:20083893; http://dx.doi.org/10.4161/epi.5.1.10724
32. Bibikova M, Barnes B, Tsan C, Ho V, Klotzle B, Le JM, Delano D, Zhang L, Schroth GP, Gunderson KL, et al. High density DNA methylation array with single CpG site resolution. Genomics 2011; 98:288-95; PMID:21839163; http://dx.doi.org/10.1016/j.ygeno.2011.07.007
33. Dedeurwaerder S, Defrance M, Bizet M, Calonne E, Bontempi G, Fuks F. A comprehensive overview of Infinium HumanMethylation450 data processing. Brief Bioinformat 2013; PMID:23990268; http://dx.doi.org/10.1093/bib/bbt054
34. Wang D, Yan L, Hu Q, Sucheston LE, Higgins MJ, Ambrosone CB, Johnson CS, Smiraglia DJ, Liu S. IMA: an R package for high-throughput analysis of Illumina's 450K Infinium methylation data. Bioinformatics 2012; 28:729-30; PMID:22253290; http://dx.doi.org/10.1093/bioinformatics/bts013
35. Izzi B, Decallonne B, Devriendt K, Bouillon R, Vanderschueren D, Levtchenko E, de Zegher F, Van den Bruel A, Lambrechts D, Van Geet C, et al. A new approach to imprinting mutation detection in GNAS by Sequenom EpiTYPER system. Clin Chim Acta 2010; 411:2033-9; PMID:20807523; http://dx.doi.org/10.1016/j.cca.2010.08.034
36. Izzi B, Francois I, Labarque V, Thys C, Wittevrongel C, Devriendt K, Legius E, Van den Bruel A, D'Hooghe M, Lambrechts D, et al. Methylation defect in imprinted genes detected in patients with an Albright's hereditary osteodystrophy like phenotype and platelet Gs hypofunction. PloS one 2012; 7:e38579; PMID:22679513;http://dx.doi.org/ 10.1371/journal.pone.0038579
37. Izzi B, Binder AM, Michels KB. Pyrosequencing evaluation of widely available bisulfite conversion methods: considerations for application. Med Epigenet 2014; 2:28-36; PMID:24944560
38. Frosst P, Blom HJ, Milos R, Goyette P, Sheppard CA, Matthews RG, Boers GJ, den Heijer M, Kluijtmans LA, van den Heuvel LP, et al. A candidate genetic risk factor for vascular disease: a common mutation in methylenetetrahydrofolate reductase. Nat Genet 1995; 10:111-3; PMID:7647779; http://dx.doi.org/10.1038/ng0595-111
39. Baek SJ, Yang S, Kang TW, Park SM, Kim YS, Kim SY. MENT: methylation and expression database of normal and tumor tissues. Gene 2013; 518:194-200; PMID:23219992; http://dx.doi.org/10.1016/j.gene.2012.11.032
40. M W. The Zebrafish Book. University of Oregon Press, Eugene, OR 1995.
41. Kimmel CB, Ballard WW, Kimmel SR, Ullmann B, Schilling TF. Stages of embryonic development of the zebrafish. Dev Dyn 1995; 203:253-310; PMID:8589427; http://dx.doi.org/10.1002/aja.1002030302
42. Krauss S, Johansen T, Korzh V, Moens U, Ericson JU, Fjose A. Zebrafish pax[zf-a]: a paired box-containing gene expressed in the neural tube. EMBO J 1991 10:3609-19; PMID:1718739